

Zeitschrift: Helvetica Physica Acta
Band: 24 (1951)
Heft: V

Artikel: The Deuteron Photo-Disintegration by the Lithium Gamma-rays
Autor: Wäffler, H. / Younis, S.
DOI: <https://doi.org/10.5169/seals-112228>

Nutzungsbedingungen

Die ETH-Bibliothek ist die Anbieterin der digitalisierten Zeitschriften auf E-Periodica. Sie besitzt keine Urheberrechte an den Zeitschriften und ist nicht verantwortlich für deren Inhalte. Die Rechte liegen in der Regel bei den Herausgebern beziehungsweise den externen Rechteinhabern. Das Veröffentlichen von Bildern in Print- und Online-Publikationen sowie auf Social Media-Kanälen oder Webseiten ist nur mit vorheriger Genehmigung der Rechteinhaber erlaubt. [Mehr erfahren](#)

Conditions d'utilisation

L'ETH Library est le fournisseur des revues numérisées. Elle ne détient aucun droit d'auteur sur les revues et n'est pas responsable de leur contenu. En règle générale, les droits sont détenus par les éditeurs ou les détenteurs de droits externes. La reproduction d'images dans des publications imprimées ou en ligne ainsi que sur des canaux de médias sociaux ou des sites web n'est autorisée qu'avec l'accord préalable des détenteurs des droits. [En savoir plus](#)

Terms of use

The ETH Library is the provider of the digitised journals. It does not own any copyrights to the journals and is not responsible for their content. The rights usually lie with the publishers or the external rights holders. Publishing images in print and online publications, as well as on social media channels or websites, is only permitted with the prior consent of the rights holders. [Find out more](#)

Download PDF: 13.12.2025

ETH-Bibliothek Zürich, E-Periodica, <https://www.e-periodica.ch>

The Deuteron Photo-Disintegration by the Lithium Gamma-rays

by H. Wäffler*) and S. Younis**)

Swiss Federal Institute of Technology, Zurich.

(17. VIII. 1951.)

Summary. The photo-disintegration of the Deuteron by the gamma-rays arising from the reaction $\text{Li}^7(p, \gamma)\text{Be}^8$ ($h\nu = 17.6$ and 14.8 MeV) has been investigated using the photographic plate technique. The angular distribution of the emitted photoprotons as well as the total cross section of the reaction have been determined. From a total of 2000 observed tracks, we obtained the following results, for both gamma-lines together:

- (1) The angular distribution in the centre-of-mass system is of the form

$$0.12 + \sin^2 \Theta (1 + 0.24 \cos \Theta)$$

It confirms within the limits of error the retardation effect calculated by MARSHALL and GUTH.

- (2) The total cross-section has the value

$$\sigma_{\text{tot}} = (8.34 \pm 1.0) \times 10^{-28} \text{ cm}^2$$

A discussion of these results from the point of view of Meson Theory of Nuclear forces is given.

Zusammenfassung. Die Photospaltung des Deutons wird mittels der im Prozess $\text{Li}^7(p, \gamma)\text{Be}^8$ emittierten Gammastrahlung ($h\nu = 17,6$ und $14,8$ MeV) untersucht. Zur Bestimmung der Winkelverteilung und des Wirkungsquerschnitts dieser Reaktion wird die photographische Methode benützt. Aus einer Statistik von 2000 Spuren ergeben sich für die Gesamtstrahlung (beide Linien zusammen) die folgenden Resultate:

1. Die Winkelverteilung im Ruhesystem des Deutons hat die Form

$$0,12 + \sin^2 \Theta (1 + 0,24 \cos \Theta)$$

Dieselbe liefert innerhalb der Fehlergrenzen eine Bestätigung des von MARSHALL und GUTH berechneten Retardierungseffekts.

2. Der gesamte Wirkungsquerschnitt beträgt

$$\sigma_{\text{tot}} = (8,34 \pm 1,0) \times 10^{-28} \text{ cm}^2$$

Die Resultate werden vom Standpunkt der Mesontheorie diskutiert.

*) Now at the University of Zurich.

**) Now at the Farouk University, Alexandria, Egypt.

1. Introduction.

The photo-fission of the deuteron is one of the fundamental experiments from the point of view of the nuclear force theory. Since its experimental discovery by CHADWICK and GOLDHABER¹), using the 2.62 MeV ThC'' gamma rays, measurements of the total cross-section and the angular distribution of the ejected nucleons for different gamma ray energies are now in progress²). For theoretical reasons, the deuteron photo-disintegration by high energy gamma rays ($h\nu \gg \varepsilon$, ε = deuteron binding energy) is of a special interest, since in this case the results of the different meson theories of the nuclear forces show quite greater deviations than those predicted at lower energies. Experiments with high energies should give information about:

(1) The constants (range and shape of potential) for the $N-P$ interaction.

(2) The ratio of ordinary to exchange forces. (Both (1) and (2) follow mainly from the total cross section of the reaction).

(3) The presence of noncentral forces in the $N-P$ system (mainly out of the angular distribution of the emitted particles).

Until recently, the generally accepted angular distribution of the ejected nucleons in the rest system of the deuteron was given by: $A + \sin^2 \Theta$ where Θ is the angle between the direction of the incoming gamma ray and the direction of motion of the emitted particle and A is a constant ranging between 0.01 and 0.44 for 17.5 MeV gamma ray energy, depending upon the type of the interaction assumed. Recent calculations by MARSHALL and GUTH³), taking into account the finite extension of the deuteron charge, give for the distribution: $A + \sin^2 \Theta (1 + 2 \beta^* \cos \Theta)$ where

$$\beta^* = \frac{V}{C} \cong \sqrt{\frac{h\nu - \varepsilon}{Mc^2}}$$

for the emitted nucleon.

After our preliminary results⁷)—using the well known⁸) Li-gamma rays ($h\nu = 17.6$ and 14.8 MeV)—had appeared, WILKINSON⁹) reported a value of $(7.7 \pm 0.9) \times 10^{-28} \text{ cm}^2$ for the cross section at 17.6 MeV. FULLER¹⁰) gave $9 \times 10^{-28} \text{ cm}^2$ for the cross-section and $0.23 + \sin^2 \Theta (1 + 0.54 \cos \Theta)$ as the angular distribution in the laboratory system by the betatron gamma rays, in an energy band of 6 MeV with a mean energy of 17 MeV. Otherwise, gamma rays of lower energies have been used. Hence, it is the aim in the following work to study in further detail through improving the statistics the deuteron photo-disintegration with the already mentioned Li-gamma rays.

2. Experiment.

(a) *General Remarks.*

Because of weak intensity as well as secondary effects from the gamma rays, electronic devices are difficult to construct to suit such a study. Registering the individual photo-protons (in a Cloud Chamber or a Photographic Emulsion) facilitates the determination of the whole angular distribution at once. Since the cross-section of the photo reaction is small ($\approx 10^{-27}$ cm²), such a study with the cloud chamber will be exhaustive. RICHARDSON and EMO¹¹⁾ found 60 proton tracks in their cloud chamber from 5000 pictures using Na²⁴ gamma-rays. A determination of the cross-section in this way is difficult since the sensitive time of a cloud chamber is hard to determine. Moreover, the relative great size of the material used in a cloud chamber or an electronic device will give rise to more scattered gamma rays, possibly affecting the angular distribution.

During the last few years, quite a remarkable progress in the production of emulsions for nuclear research work¹²⁾ has been attained. It is now possible to accommodate several types of plates for such an investigation, and we believe that these plates supersede the other detecting devices owing to the ease of their handling and treatment.

By soaking the plates in heavy water till saturation⁷⁾ one obtains $\sim 2 \times 10^{23}$ Deuteron nuclei/cm³ of the emulsion. GIBSON et al.¹³⁾ reported a gain of $\sim 1.5 \times 10^{22}$ D-nuclei/cm³ by loading the plates with calcium nitrate with D₂O as water of crystallization, to study the deuteron-disintegration by Fluorine gamma-rays [$h\nu \sim 6$ MeV].

Since for the Li-gamma-rays the quantum energy $h\nu$ exceeds the mean binding energy of neutrons and protons in most nuclei, one finds¹⁴⁾ photo-protons arising from Ag, Br, O... nuclei existing in the emulsion beside those from the D-nuclei [the (γ, p) cross-section on Ag and Br is about 10 times greater than that on D]. To extract the disturbing photo-protons from the whole statistics of a certain plate, another one may be soaked in H₂O, irradiated and treated exactly under the same conditions like the D₂O-plate. The difference between the two plates (D₂O — H₂O) yields the photo-protons from the D-nuclei. To minimise the statistical fluctuations of the difference, the greatest possible concentrations of D-atoms should be used.

(b) *Preparation of the Plates.*

Ilford C 2, 300 μ and 400 μ plates have been used during different runs of exposure. At every time, two plates from the same batch were cut to an area of 2.2×2.6 cm². After being weighed by a torsion balance sensitive to a fraction of 1 mg, one was immersed in H₂O and the other in D₂O during a time long enough to obtain complete saturation. This time amounts to 3 hours for the 300 μ plates (see fig. 1), after which the water excess has been removed

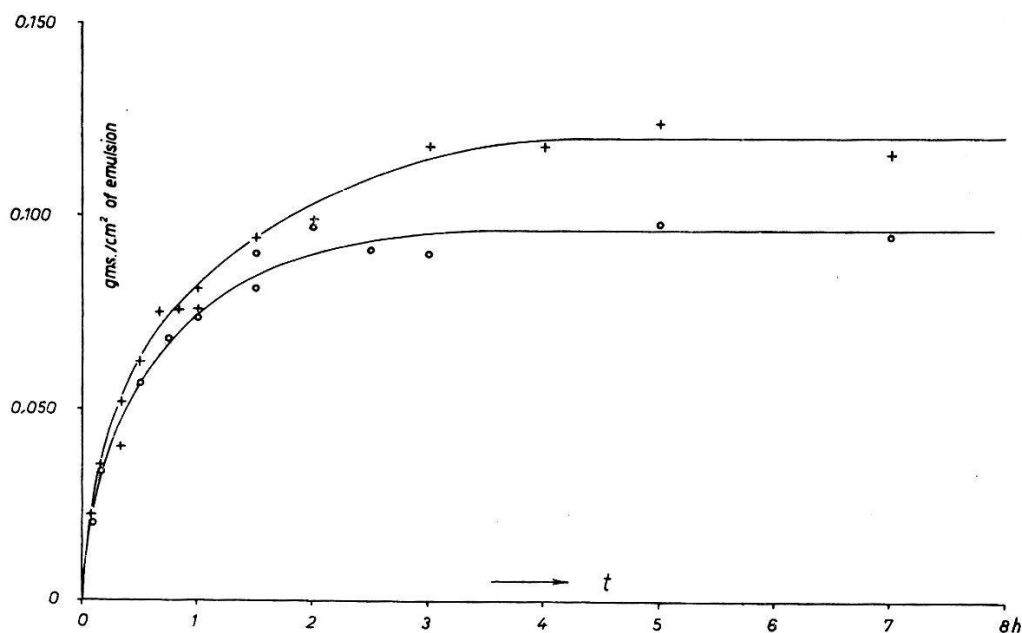


Fig. 1.

Uptake of water in the emulsion as a function of soaking time t in Ilford plates.
 + 400 μ C₂. o 300 μ C₂.

carefully from the glass, and then the plates re-weighed. For the irradiation, the wet plates were put in air tight aluminum cassettes containing a small amount of the corresponding water to ensure saturated vapour around the plates. Irradiations were performed under striking incidence as well as—for a check of eventual scattering inside the emulsion—under a glancing angle of 5°.

(c) *Apparatus and Irradiation.*

We refer to a previous work¹⁴⁾ for the description of the apparatus used for producing the Li gamma-rays. In the present work, a magnetically resolved proton beam of 200–300 μ amps, falling on a thick metallic Li-target (0.1 mm thick and 3 mm diameter) has been used. The absolute yield of gamma rays has been determined with a thick-walled aluminum-counter, using the yield-curves given

by FOWLER et al.¹⁵). The target support was cooled by a water current allowing a regulation of the temperature of the cassettes. The time of exposure was usually limited to several hours (4 to 5 h), to avoid the fading of tracks and the fogging of plates which disturb the observations⁷). Fig.

2 shows the target-cassettes arrangement for the irradiation. The plates have been weighted just after the end of irradiation and then immediately developed. Only those plates which showed a change of less than 2% in the water contents during the exposure, have been used for evaluation.

(d) *Treatment of the Plates.*

Proton tracks in wet emulsions appear generally weaker, than in dry (for a comparison, see photographs in reference 7). This difficulty, however, can be greatly overcome by appropriate treatment. The best one we have found for Ilford C₂ 300 μ plates is the following:

(1) Wash in running water for a short time.

(2) Soak in Ilford ID-19 (1:3 by volume) at 4° C for 90 minutes with no agitation.

(3) Change in ID-19 (1:3 by volume) at 18° C for 40 minutes with rocking the container.

(4) Wash in running water for half a minute.

(5) Soak in a cool acid hardener during 20 minutes with slight rocking.

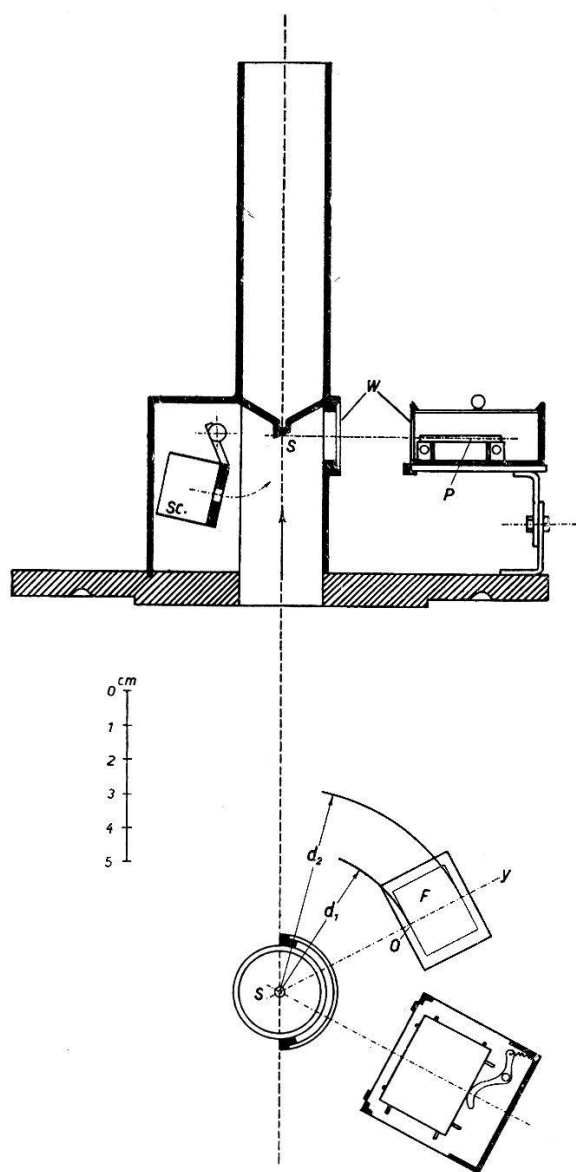


Fig. 2.

Arrangement for irradiation of photographic plates.

S = Li-target 3 mm diameter; Sc = Screen; P = Photographic Plate; F = Scanned area on the plate; $SO = d_1$ = fixed distance from source = 43 mm; $W = 0,1$ mm Al-Window.

(6) Wash in water for half a minute.

(7) Fix in a 30% sodium thiosulfate neutral solution at 20° C with strong agitation. The fixer should be changed periodically each $\frac{1}{2}$ hour. During the change, the plates are washed in running water. Fixation should be continued during $1.5 \times$ the necessary time till the plates are apparently clear (~ 6 hours).

(8) Wash in cool running water at least two hours.

(9) Leave to dry slowly in a dust free room.

(e) *Marking the Plates.*

After being treated and dried, the plates—in their corresponding cassettes—were again brought to their exact position relative to the source as during the irradiation. An arc of 43 mm radius, whose centre of curvature coincides exactly with the central point of the source S has been marked on each plate's surface. A line OY , passing through the centre of the source and perpendicular to the plate's edge facing the target, was also marked with its extension on the emulsion's surface (see figure 2). In the microscopie evaluation, the plate was fixed on a slide frame in such a position, that the marked line OY observed in the field of view moves just parallel to the perpendicular movement of the table's scale of the microscope.

(f) *Measurements Technique.*

Three Leitz binocular "Research Microscopes", each fitted with a mechanical stage, were used. Verniers on the stage, with least count 0.1 mm allowed easy resetting on a track. Apochromatic oil immersion objectives (N. A. 1.15, 3 mm, $60 \times$) together with pairs of $5 \times$ periplan eyepieces were used for searching tracks. Such an optical system gives a fairly small depth of focus. The area of the examined plate was scanned in horizontal strips manipulated by the mechanical stage. To avoid the remeasuring of the same track, settings of the mechanical stage on the track's beginning were used as its coordinates and recorded beside its other measurements. Measurements of the tracks' projection l' were accomplished by the use of a $6 \times$ eyepiece scale, calibrated by reference to an objective micrometer. (The mean error in l' amounts to $\pm 3\%$). The dip h of the track in the emulsion was measured by a vertical vernier-micrometer gauge (exact to $\pm 0.5 \mu$). The projection angle between

the tracks' beginning and the perpendicular axis OY was read (up to a maximum error of $\pm 0.5^\circ$) with the help of a pointer fixed to the measuring eyepiece and rotating on a goniometer graduated in degrees. From each run of irradiation, two areas on the D_2O - and H_2O -plates, identical with respect to the target were examined. All tracks lying entirely in the emulsion were noted and measured.

3. Treatment of the data.

(a) *Shrinkage Determination.*

In order to compute the true length and angle of dip of each track, it is necessary to establish the exact relationship between its orientation during exposure and that after processing. This relationship is determined by the shrinkage S of the emulsion, which is defined by the ratio

$$S = \frac{\text{thickness at exposure}}{\text{thickness after processing}}$$

The mean value of shrinkage could be determined directly by measuring the emulsion thicknesses of a test plate by means of a micrometer gauge before and after treatment. In our case, the shrinkage factor depends upon the water contents and the way of treatment. Thus, we have had to determine it for each individual plate under examination. This has been done by measuring the photo protons—under different inclinations—from the reaction $O^{16}(\gamma, p)N^{15}$ which have shown a group with a maximum at 5.15 MeV^{16} .

The true length of a track is given by $l = \sqrt{l'^2 + h^2 S^2}$, where l' and h are its horizontal- and vertical-projections respectively and S is the shrinkage. We transform the above relation into a linear one by plotting l'^2 against h^2 , assuming the tracks to have all the same length l since they belong to the same reaction. By the least square method one can draw the most suitable straight line through the points whose inclination $= -1/S^2$ (see fig. 3). By this method, the mean relative error in S has been found to be $\pm 6\%$.

The usual way to correct for shrinkage is to multiply the vertical projection of the track-length by the mean shrinkage factor of the emulsion. This is based on the assumption that the shrinkage all over the depths affects all tracks in a uniform manner; but this is not immediately obvious, owing to the complicated phenomena which occur at processing. ROTBLAT and TAI¹⁷⁾ found that the shrinkage factor S is the same for different layers of the dry emulsion. To realise this result in wet emulsions we have soaked a 400μ

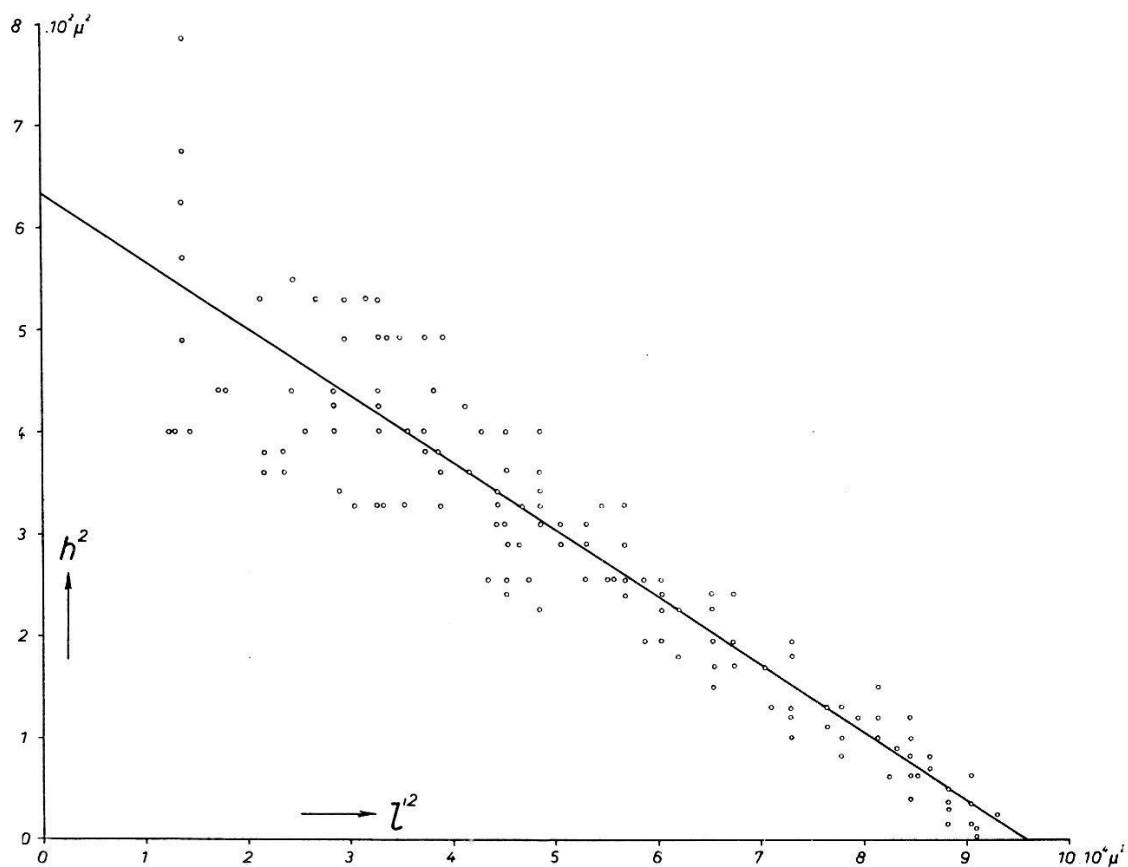


Fig. 3.

l'^2 against h^2 for tracks from the reaction $\text{O}^{16}(\gamma, p) \text{N}^{15}$ in a wet 300μ plate.
 $S = 12.5 \pm 0.7$.

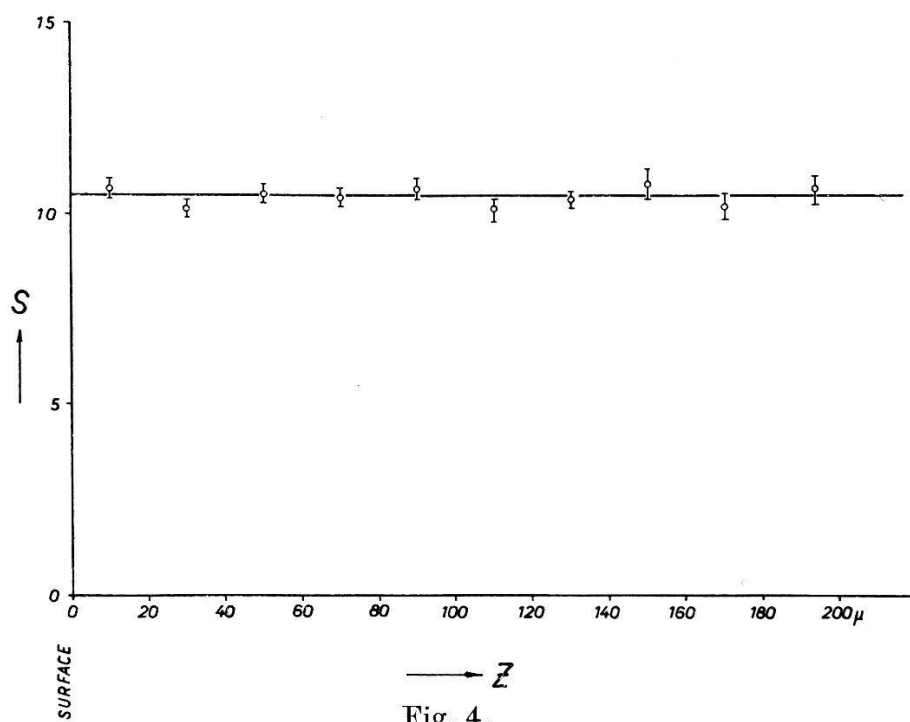


Fig. 4.

Shrinkage as a function of depth Z in a wet 400μ plate.

C 2 plate in a neutral Po-solution and treated it in the usual way. The measurements of the alpha-tracks in different layers were carried out and the mean shrinkage value for each layer was determined as mentioned above. From fig. 4 which gives a relation between the values of S as a function of the layer depth, it can be concluded that S is practically the same all over the emulsion thickness. Taking into account the error in the measurements of the projection length and height of a track $\Delta l'$, Δh mentioned under part 2, together with the error of shrinkage (ΔS), one can calculate

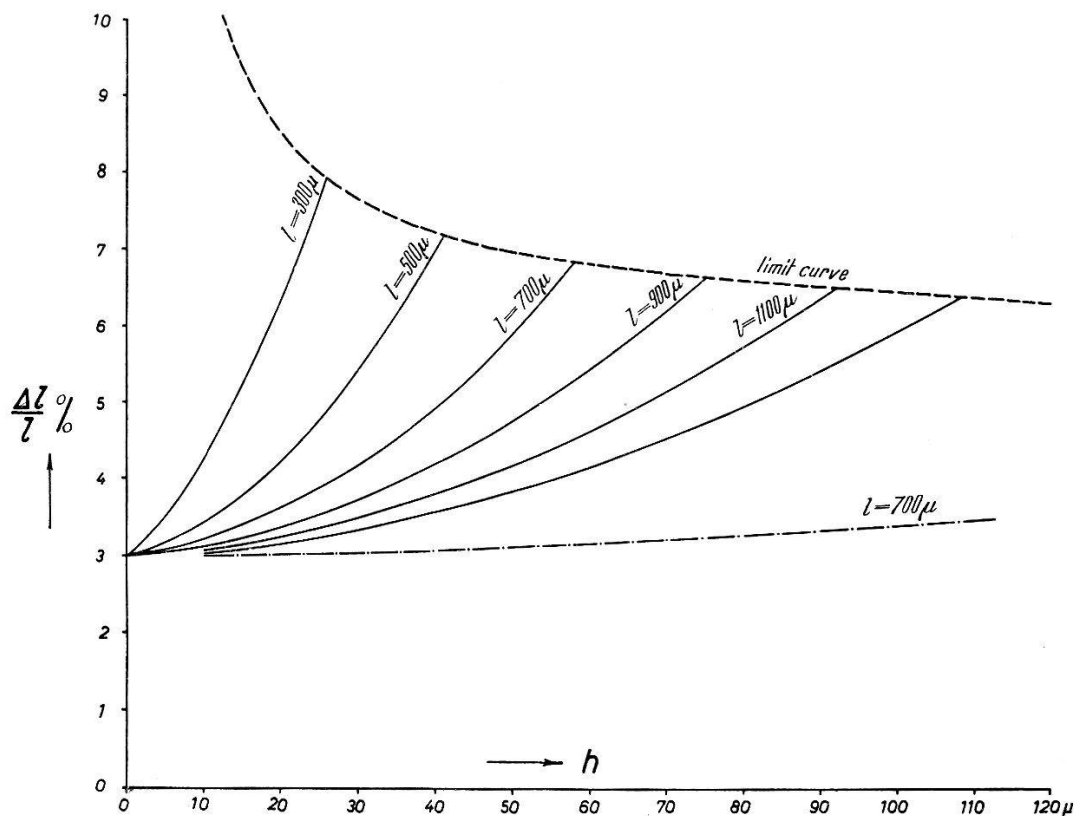


Fig. 5.

Variation of the relative error in true length with the height. Notice that for a given fixed l the error will not exceed a certain value determined by the dashed curve.

- wet emulsion (shrinkage $S = 12$)
- - - - dry emulsion, for comparison ($s = 2.5$).

the relative error in the determination of the track's true length l , from the formula:

$$\frac{\Delta l}{l} = \left(\frac{l'}{l}\right)^2 \cdot \left(\frac{\Delta l'}{l'}\right) + \left(\frac{hS}{l}\right)^2 \cdot \left(\frac{\Delta h}{h}\right) + \left(\frac{hS}{l}\right)^2 \cdot \left(\frac{\Delta S}{S}\right).$$

Figure 5 shows as an example the relation between $(\Delta l/l)$ and h with l as a parameter in a wet plate assuming a shrinkage of 12.0. From this figure one concludes that steep tracks have greater relative error in their true lengths than flat ones in the same plate.

It may be mentioned that the deviations of true lengths from the mean in a wet plate are greater than those in a dry one (assuming $S=2.5$ and the same relative errors in measurements like in the wet plates). This shows that the straggling of the proton ranges in wet emulsions is greater than those in dry ones. It is furthermore clear

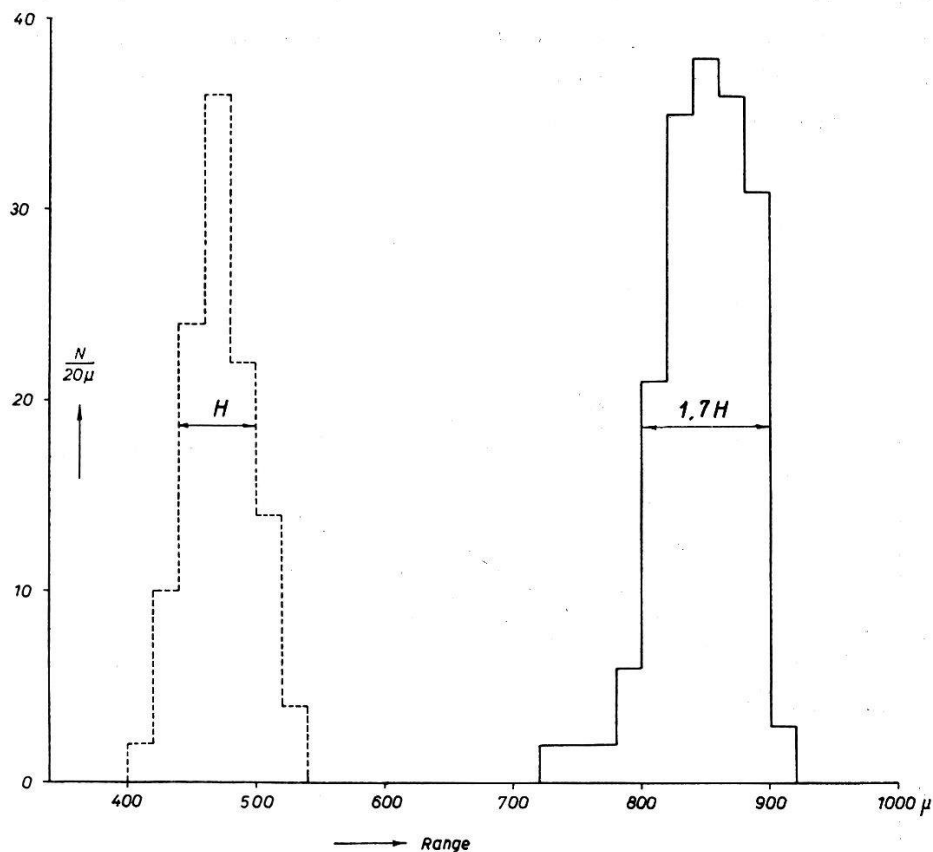


Fig. 6.

Range distribution of 9 MeV recoil protons ($C \approx 100 \mu$).

- in a wet plate (180 tracks, uptake of $H_2O = 22 \text{ mg/cm}^2$).
- in a dry plate (120 tracks).

from figure 6, which shows a range distribution of recoil protons (scattering angle $0^\circ \pm 20^\circ$) from 9 MeV neutrons emitted in the reaction $B^{11}(d, n)C^{12}$, that the range of protons of a fixed energy in the wet emulsion is greater than in the dry.

(b) Range-Energy Determination.

To transform the ranges of the proton-tracks into an energy scale, a "range-energy" relation in the wet emulsions must be determined. To develop such a relationship, we have measured the recoil protons in wet plates exposed to $(B + D)$ — and $(Li + D)$ — neutrons produced by the above described high tension generator. The energy-spectra of the neutrons in both reactions have been recently deter-

mined by GIBSON¹⁸), GREEN and GIBSON¹⁹) and also in this laboratory²⁰). Thus several points were available for an energy-range transformation limited just to the interesting domain (3–14 MeV). As is shown in figure 7, all these points — after dividing the ranges in the wet emulsion by a constant factor f — lie exactly on the

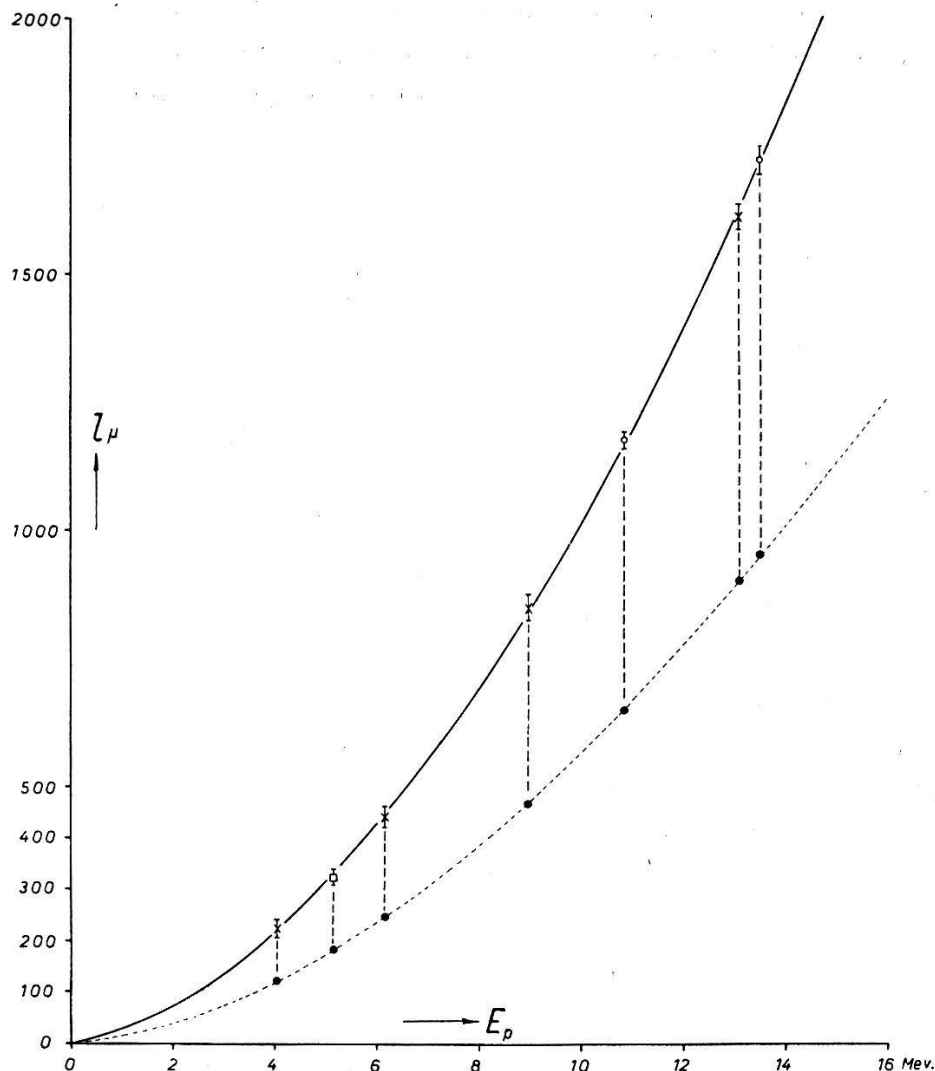


Fig. 7.

Range energy relation for protons.

- wet C₂ Ilford plate (o Li + D, x B + D, O¹⁶ (γ , p)N¹⁵; $f = 1.8$.)
- dry C₂ Ilford plate (Lattes et al.)

range energy curve determined by LATTES et al²¹). Since this lengthening depends upon the water content, the range-energy distribution has to be determined for each plate separately by determining the factor f from a calibrating point. In the case of the gamma-irradiated plates, the pronounced group from O¹⁶ (γ , p) N¹⁵ with $E_p = 5.15$ MeV¹⁶ (see also fig. 8) gives one the chance of an exact determination of f .

4. Results.

(a) Energy distribution.

Figure 8 shows the energy distribution of the photo-protons found in seven pairs of plates (D_2O and H_2O) of a total area of $2 \times 28 \text{ cm}^2$. (9200 tracks in D_2O and 7000 tracks in H_2O). The errors shown are merely statistical fluctuations. The pronounced maxima at 5.15 MeV

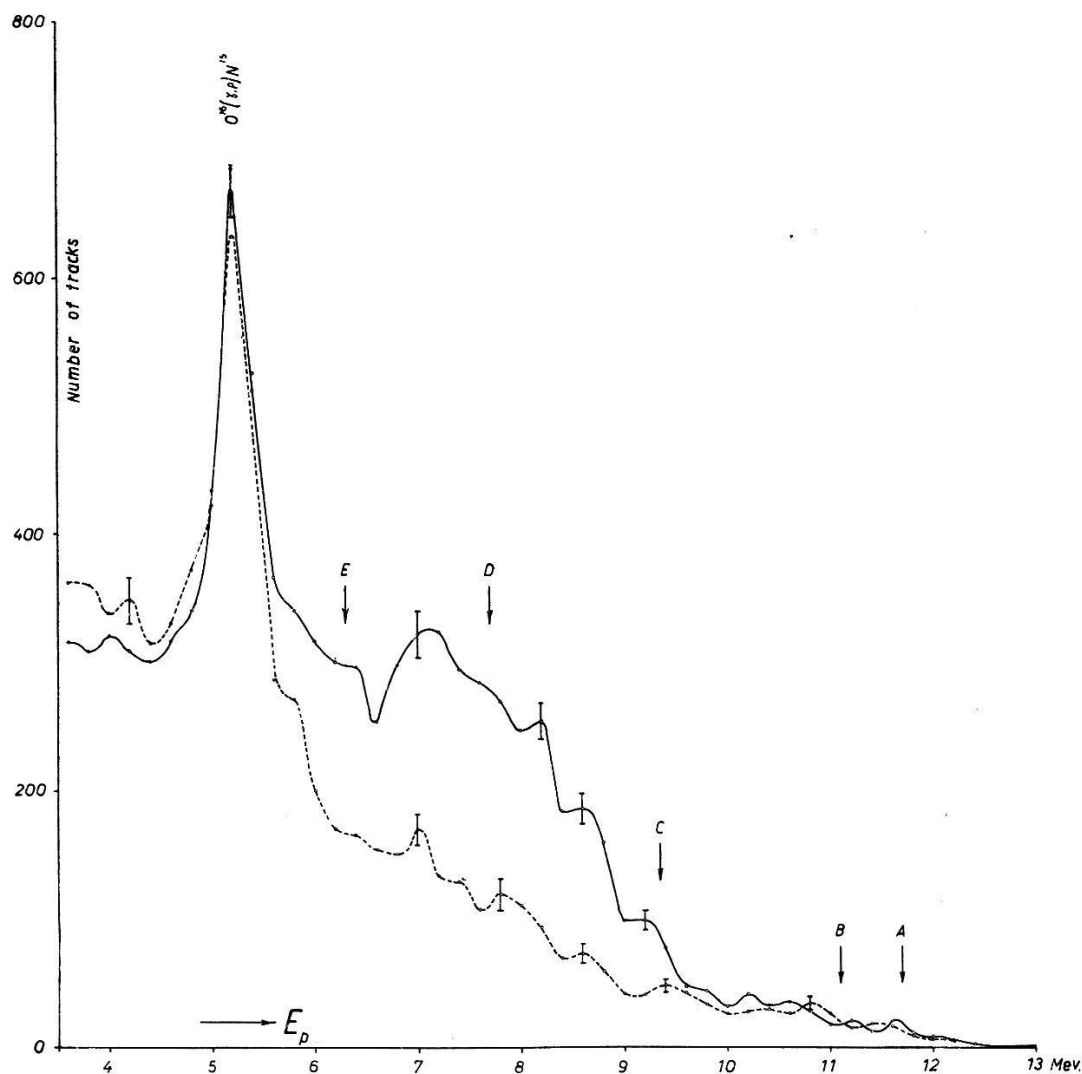


Fig. 8.

Energy distribution of the photo protons.

- in D_2O Plates (9200 tracks in 28 cm^2).
- in H_2O Plates (7000 tracks in 28 cm^2).

are attributed to protons from $O^{16} (\gamma, p) N^{15}$. Arrows A, B and C indicate the position of the photo protons of maximum energy from Ag^{107} , Br^{79} and N^{14} respectively, corresponding to a transition into

the ground state of the rest nuclei*). The D₂O-plates show an excess of tracks in a broad domain (extending from ≈ 4.8 to 9.5 MeV) over the H₂O-plates, arising from the deuteron photo-disintegration.

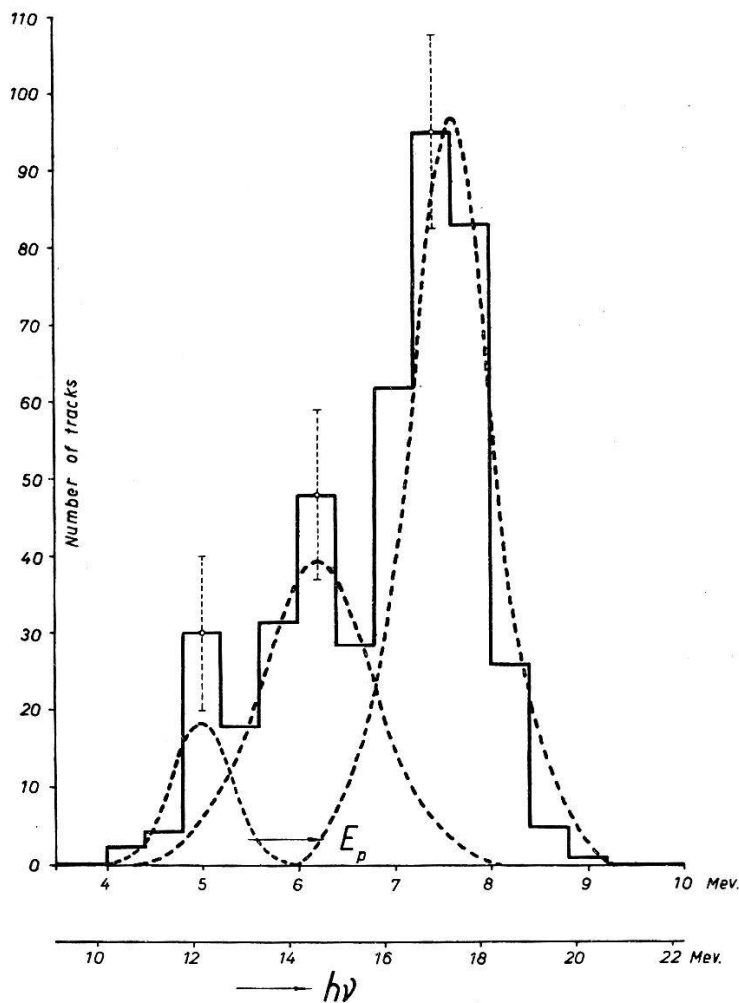


Fig. 9.

Energy distribution of 400 photo-protons, taken in a cone of half-opening of 30°, with axis perpendicular to the incoming gamma-rays.

Lower scale: gamma-ray energy producing these protons ($h\nu \cong 2 E_p + \varepsilon$). Steps taken in intervals of 0.4 MeV. The vertical dotted lines give the mean statistical error.

For the deuteron photo-disintegration, the energy of the emitted proton in the center-of-mass system of the deuteron is given by

$$E_p (\text{C.-M.}) = \frac{1}{2} (h\nu - \varepsilon)$$

($\varepsilon = 2.23$ MeV: binding energy of the Deuteron)

*) The proton binding energies in Ag¹⁰⁷ and Br⁷⁹ (5.7 and 6.5 MeV respectively), are given by B. C. DIVEN and G. M. ALMY, Phys. Rev. **80**, 407 (1950).

For N¹⁴ it was calculated from the masses to be = 7.6 MeV. (Isotopic Report by J. MATTAUCH and A. FLAMMERSFELD, Tübingen (1949)).

and in the laboratory system by

$$E_p(\text{lab.}) = \frac{E}{2} - \frac{(\hbar\nu)^2}{4Mc^2} \left[\sin^2\Theta - \cos\Theta \sqrt{\cos^2\Theta - 2 + \frac{4Mc^2}{(\hbar\nu)^2} \cdot E} \right]$$

where $E = \hbar\nu - \varepsilon$ and Θ is the angle of emission in the same system.

This means, protons under different angles from the 17.6 MeV and 14.8 MeV groups would interfere in an energy scale. Calculated energies of photo protons from deuteron disintegration under different angles of emission would give a continuous distribution spread in a region from 5.4 to 9.0 MeV with two maxima at 7.7 and 6.3 MeV indicated by arrows *D* and *E* in figure 8. Figure 9 gives the energy distribution of 400 protons from the difference ($\text{D}_2\text{O} - \text{H}_2\text{O}$) in a cone with axis at 90° with respect to the incoming rays and a half opening of 30° . This choice has been considered simply because at this axis, the gamma-ray energy is given very nearly by:

$$\hbar\nu = 2E_p + \varepsilon.$$

With a greater cone opening, the variation of energy of protons with the angle Θ is remarkable; besides, for steep tracks the shrinkage causes greater uncertainties in the energy determination (see e. g. figure 5).

One sees clearly from figure 9 three main gamma-ray lines from $\text{Li}^7 + p$ above 10 MeV, namely,

17.6 MeV (arising from $\text{Be}^{8*} \rightarrow 2\alpha + \hbar\nu$ into the ground state);

14.8 MeV (arising from $\text{Be}^{8*} \rightarrow 2\alpha + \hbar\nu$ into the 2.8 MeV excited state);

and ≈ 12.2 MeV (arising from $\text{Be}^{8*} \rightarrow 2\alpha + \hbar\nu$ into an ≈ 5.0 MeV excited state).

To obtain the number of quanta J , which belong to each line, the histogram was fitted by the gaussian distribution (dotted curves in fig. 9). Assuming the deuteron photo-disintegration cross section to be proportional to $\frac{(\hbar\nu - \varepsilon)^{3/2}}{(\hbar\nu)^3}$ a good approximation for higher quantum energies ($\hbar\nu \gg \varepsilon$), the histogram gives us for the number of quanta the ratios:

$$J(17.6):J(14.8):J(12.2) = 1:0.45:0.08$$

Thus, our intensity ratio for the two main lines is in good agreement with the results of WALKER and McDANIEL²²), who give the value 0.5 for this ratio. The third (≈ 12.2 MeV) line has not been reported before and cannot be considered as definitely established. Never-

theless, experimental evidence from the reaction discussed here as well as from the carbon-photodisintegration²⁷) seems convincing enough to us to consider the presence of a third line in the lithium gamma spectrum as rather probable. For the calculation of the total cross section (section C) this line has therefore been taken into account in the computation of the absolute number of quanta. Before we go on to discuss the results, we shall try to mention the disturbing effects and how to eliminate them.

(1) *The Neutron Background.*

By irradiating Li with a magnetically resolved proton beam, practically no (Li + D) neutrons come into question. The main source of neutrons from the target is the $\text{Li}^7 (\alpha, n) \text{B}^{10}$ reaction. They have a maximum energy of 4.68 MeV. Under the present irradiation conditions, it was calculated that the plates receive a flux of about 50 neutrons per sec per cm^2 . The possible effect of these neutrons in the plates influencing the difference between the D_2O and H_2O measurements is the production of recoil protons (or deuterons), but by limiting the measurements to angles greater than 40° , these recoils are so short that they will have no interference in the measured protons. The $\text{D} (n, 2n) \text{p}$ reaction in the D_2O plates is theoretically possible, but owing to its very small cross section (≈ 0.05 barns), this effect does not play any role in our measurements.

(2) *The absorption of gamma-rays in the emulsion.*

For a calculation of the total cross section of the deuteron photo-disintegration, the absorption of the gamma rays in the emulsion must be taken into account. Assuming an exponential absorption law, the number of measured tracks as a function of the distance d from the source is given by

$$N(d)_{\text{exp}} = N_0 \frac{e^{-\mu(d-d_1)}}{d^2}$$

d_1 = distance from the source to the edge of the plate.

To determine the absorption coefficient μ , in Fig. 10 $\log (N \cdot d^2)$ is plotted against d . The inclination of the straight line, drawn by a least square fit through the experimental points, gives us the absorption coefficient μ , namely $\mu = 0.072 \text{ cm}^{-1}$. From this, by a development in series, one gets for the effective number of tracks

$$N_{\text{eff}} = N_{\text{exp}} \frac{1}{1 - \mu d_1 \left\{ \frac{d_2}{d_2 - d_1} \ln \left(\frac{d_2}{d_1} \right) - 1 + \dots \right\}} \cong 1.07 N_{\text{exp}}$$

(b) *The angular distribution and the isotropic constant A .*

Owing to the finite distance between the plates and the source, a correction in the projection angle should be applied to each track (γ -rays passing through the plate are not parallel). This correction has been done by plotting the tracks with respect to the source on a $20 \times$ scale. If Φ is the correct projection angle between a ray and a track, α is the track's angle of dip and Θ is the true angle in space between the gamma ray and the track, then:

$$\cos \Theta = \cos \alpha \cdot \cos \Phi.$$

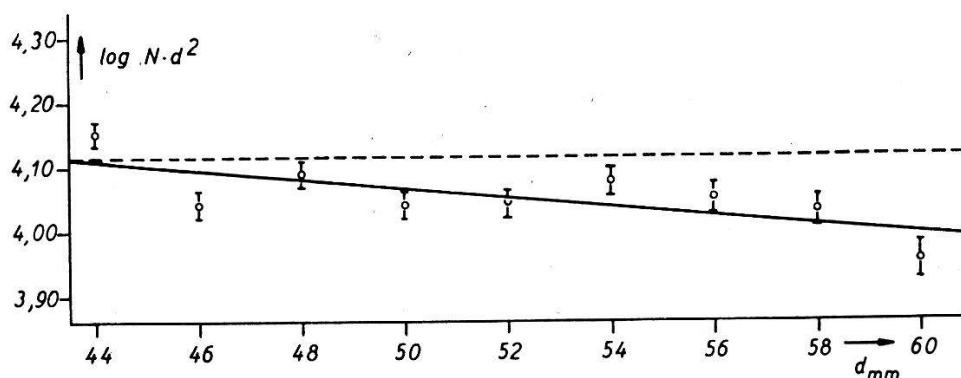


Fig. 10.

Logarithmic plot of the number N of photo protons in successive strips of 0.2 cm breadth (0.5 cm^2 area) times the square of the distance (d^2), as a function of d .

The angle Θ was calculated for each track with the help of a logarithmic nomogram. The calculated maximum error in Θ —due to the errors in shrinkage ΔS and the projection angular definition $\Delta \Phi$ (error of reading + geometrical error of finite area of source) — will not exceed 3.5° in any case. To construct the angular distribution, one must correct the number of tracks measured in an interval $\Theta - \Delta \Theta/2$ and $\Theta + \Delta \Theta/2$ for the tracks leaving the emulsion. The factor K to be multiplied by the measured number of tracks of a mean range l , is given (per unit solid angle) by:

$$K = \frac{1}{2 \sin \Theta \left(\pi - \frac{l}{H} \sin \Theta \right) \Delta \Theta} \quad \text{for } 2H \geq l \sin \Theta$$

$$K = \frac{1}{4 \sin \Theta \left[\arcsin \left(\frac{2H}{l \sin \Theta} \right) - \frac{l \sin \Theta}{2H} + \sqrt{\frac{l^2 \sin^2 \Theta}{4H^2} - 1} \right] \Delta \Theta} \quad \text{for } 2H \leq l \sin \Theta$$

where $2H$ is the thickness of the emulsion during exposure. Fig. 11

shows the variation of the escape factor with $l/2 H$ and Θ as a parameter.

The angular distribution of 2000-tracks difference between D_2O - and H_2O -plates from 14.8 and 17.6 MeV together in laboratory system is shown in figure 12. The forward distribution up to 40° is cut out to eliminate all possible neutron effects as mentioned

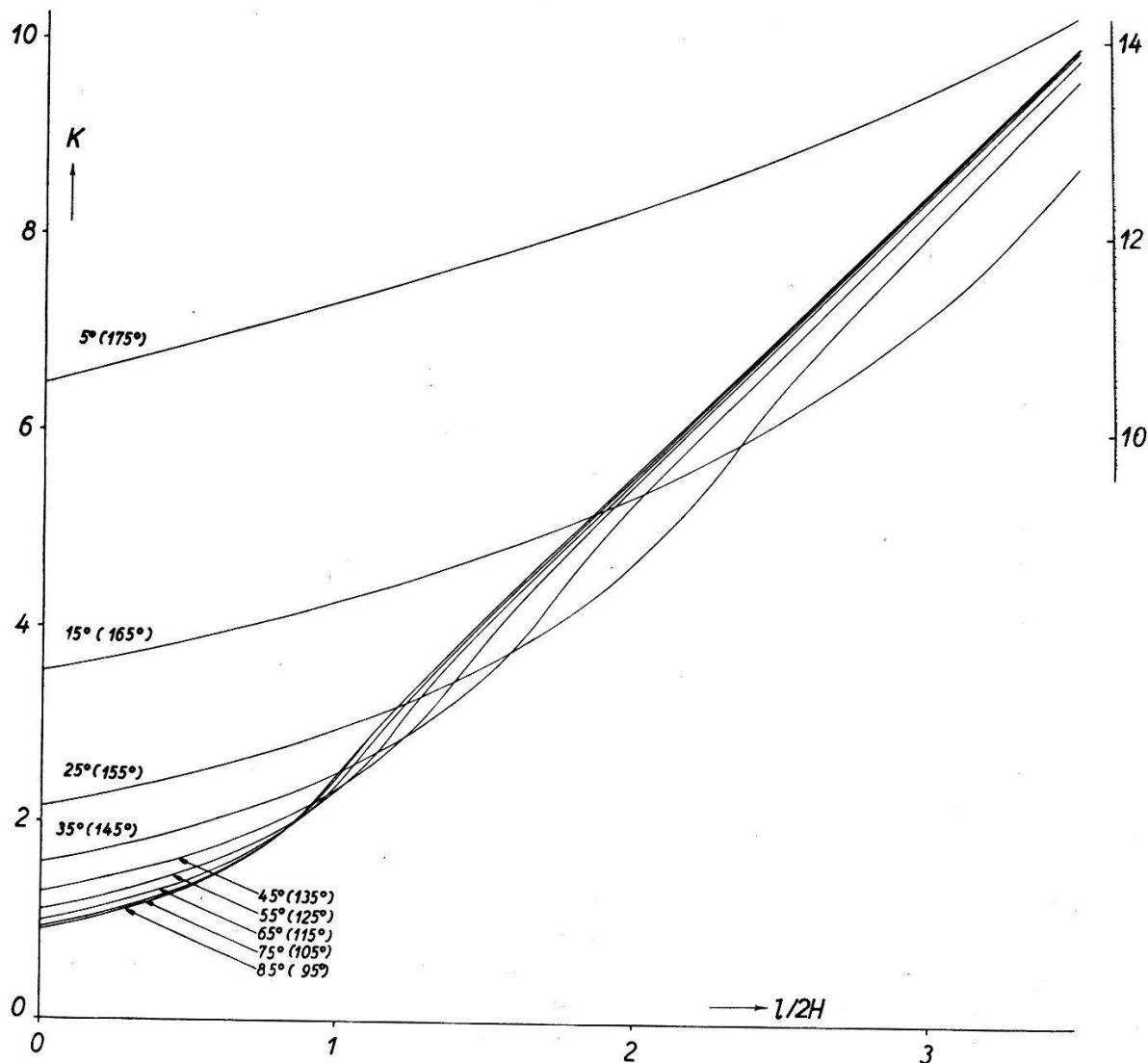


Fig. 11.

Escape factor K per unit solid angle as a function of $l/2 H$.
(Scale on right for $\Theta = 5^\circ (175^\circ)$.)

before. The experiment fits quite well with the theoretical asymmetric distribution:

$$A + \sin^2 \Theta (1 + 2 \beta^* \cos \Theta); (\beta^*: \text{retardation factor})$$

transformed in the laboratory system. In the latter case, neglecting terms of higher order, the distribution has the form:

$$A (1 + 2 \beta \cos \Theta) + \sin^2 \Theta [1 + (2 \beta^* + 4 \beta) \cos \Theta]$$

where $\beta^* \cong \sqrt{\frac{h\nu - \varepsilon}{Mc^2}}$ and $\beta = \frac{h\nu}{\sqrt{4Mc^2(h\nu - \varepsilon)}}$. For our two main gamma-lines, assuming the relative intensities $\frac{I(14.8)}{I(17.6)} = 0.45$, the calculated mean values of β and β^* are:

$$\bar{\beta} = 0.071 \text{ and } \bar{\beta}^* = 0.127$$

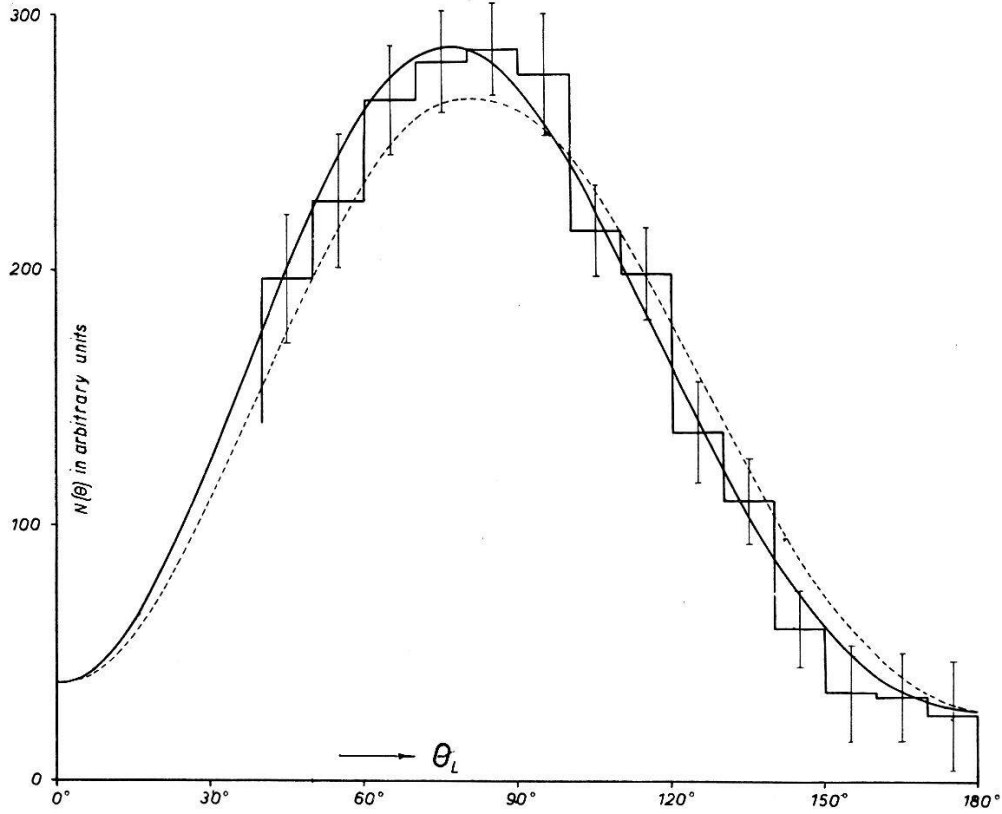


Fig. 12.

Angular distribution of the deuteron photo-disintegration for the 14,8- and 17,6-MeV gamma-rays combined (in the lab. system).

Histogram: experimental angular distribution (2000 tracks) corrected for tracks leaving the emulsion (the number of tracks per unit solid angle is given). The length of the vertical lines indicates the standard statistical error.

Curves: The equal area fit to the histogram between the limits $40^\circ \leq \theta \leq 180^\circ$.

..... symmetric form $\sigma(\theta) \sim 0.1(1 + 0.142 \cos \theta) + \sin^2 \theta(1 + 0.284 \cos \theta)$.

—— asymmetric form $\sigma(\theta) \sim 0.1(1 + 0.142 \cos \theta) + \sin^2 \theta(1 + 0.538 \cos \theta)$.

For a more quantitative comparison between the theoretical curves and the histogram, the parameters A and β^* in the distribution assumed to be of the form

$$A(1 + 0.142 \cos \theta) + \sin^2 \theta [1 + (2\beta^* + 0.284) \cos \theta]$$

have been calculated from the histogram by the method of the least squares.

The result of this computation is

$$A = 0.096 \quad \beta^* = 0.119,$$

β^* being in close agreement with the mean theoretical value (0.127).

Another determination of the isotropic constant A , which is independent from the assumed value for the retardation factor β^* , can be obtained by “folding” the angular distribution around the 90° -direction:

$$\Phi(\Theta) \equiv \sigma(\Theta) + \sigma(180^\circ - \Theta) \sim A + \sin^2 \Theta$$

If we plot $\Phi(\Theta)$ against $\sin^2 \Theta$, averaged in an interval $\Delta\Theta = 10^\circ$, then we obtain a straight line fitting the points whose intercept with the negative $\sin^2 \Theta$ -axis gives A . By an application of the least square method to the experimental points we found (see fig. 13) for the 14.8 and 17.6 MeV components together:

$$A = 0.10 \pm 0.05 \text{ (mean statistical error)}$$

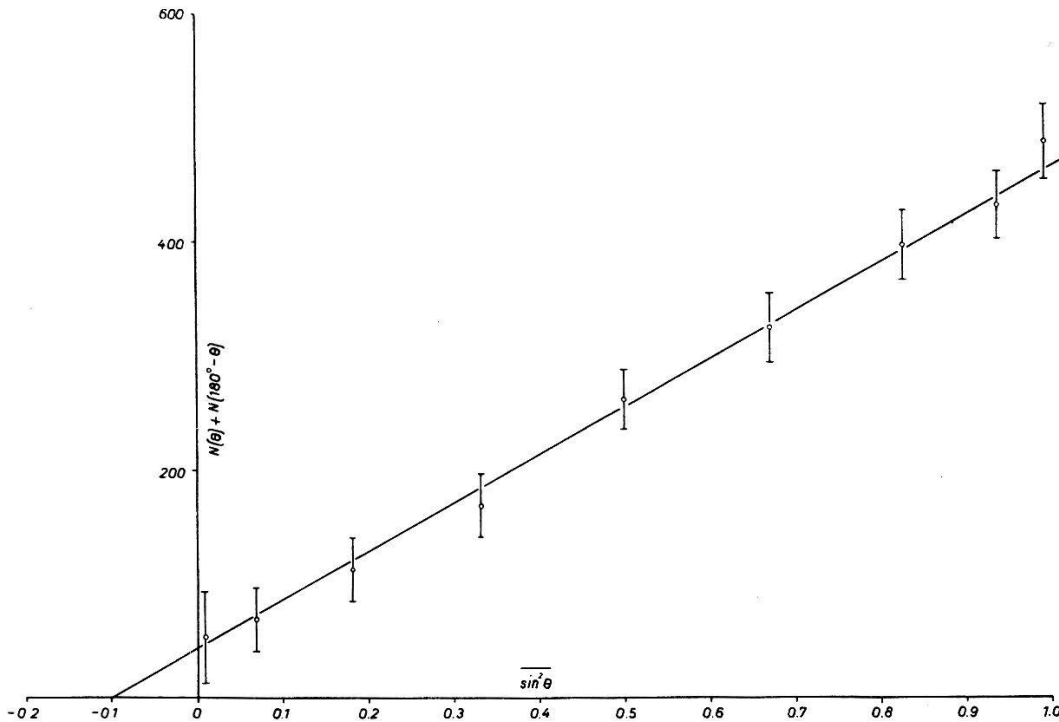


Fig. 13.

Distribution of deuteron photo-protons by 14,8 and 17,6 MeV lines together.
(The whole distribution is folded around 90° and plotted against $\sin^2 \Theta$.)

A third determination of A , which is practically free from errors introduced by escape corrections, can be obtained by accepting only those tracks, which (in the lab. system) lie inside rotation cones around the 90° —and 180° —directions (say N_2 and N_1 tracks respectively) with the same vertex angle 2ψ . One can show with the

use of the angular distribution that the isotropic constant A is calculated by the formulae:

$$A = \frac{R[(1-\cos \psi) + \frac{1}{3}(1-\cos^3 \psi)] - [(1-\cos \psi) - (\beta^* + 2\beta)(1-\cos^2 \psi) - \frac{1}{3}(1-\cos^3 \psi) + (\beta + \frac{1}{2}\beta^*)(1-\cos^4 \psi)]}{[1 - 2R - \beta(1 + \cos \psi)](1 - \cos \psi)}$$

and the mean standard error in A with a fixed measured total number of tracks is given by

$$\delta A = \frac{(2\alpha + f)[\alpha - \alpha\beta(1 + \cos \psi) - f + V]^{\frac{1}{2}} + [\alpha - \alpha\beta(1 + \cos \psi) - f + V](2\alpha + f)^{\frac{1}{2}}}{\sqrt{1 - \cos \psi}[3f - \beta f(1 + \cos \psi) - 2V]}$$

$$\text{where } \alpha = A + \frac{2}{3},$$

$$f = \frac{1}{3} \cos \psi (1 + \cos \psi),$$

$$V = \frac{-\left(\beta^* + \frac{4}{3}\beta\right)(1 - \cos^2 \psi) + \left(\frac{\beta^*}{2} + \beta\right)(1 - \cos^4 \psi)}{1 - \cos \psi}$$

$$\text{and } R = N_1/2 N_2$$

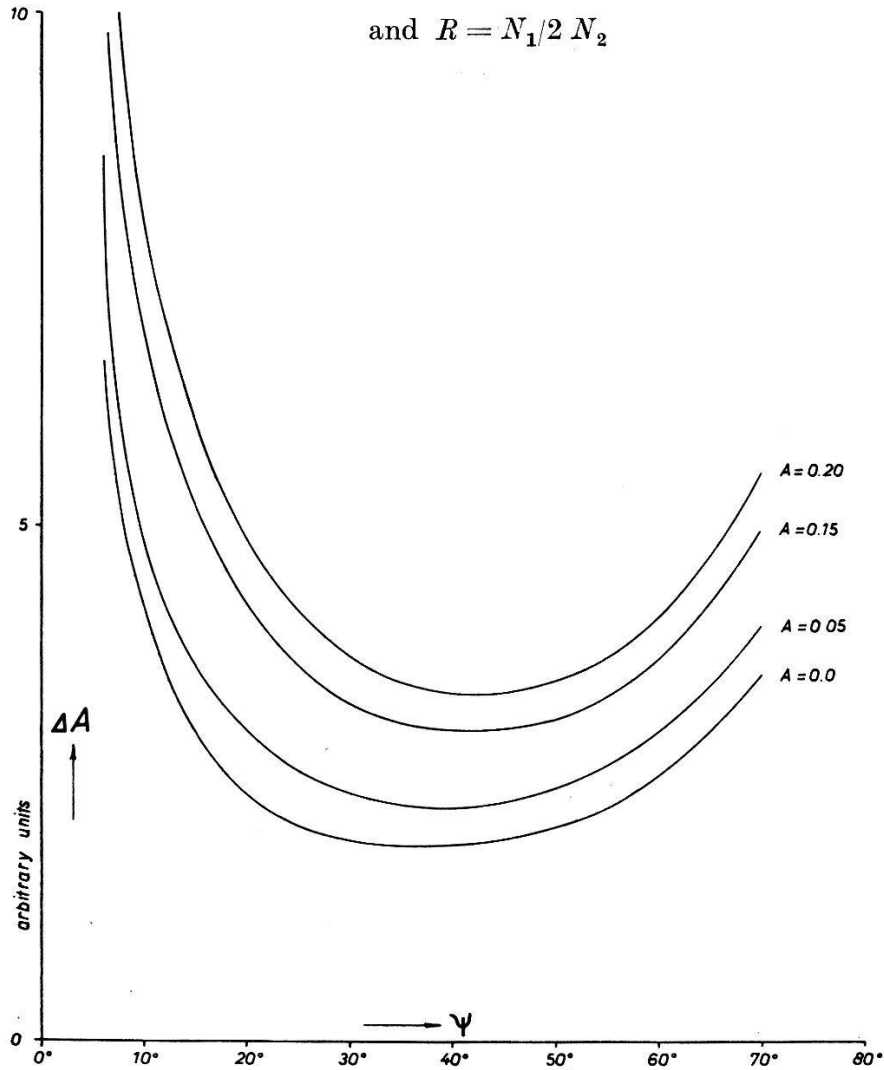


Fig. 14.

Error in the isotropic constant A with cone's opening-angle ψ for a constant number of measured tracks (A is taken as a parameter).

The factor $1/2$ in R arises from the fact that we have considered the two 90° -cones, namely the left- and right-hand sides. Figure 14 shows the error in A as a function of the opening angle 2ψ with a constant total measured number of tracks. One sees that δA is a minimum with a certain optimum angle ψ of the cones for a fixed A . By choosing $\psi = 30^\circ$ in our measurements, we have found $N_1 = 29 \pm 12$ tracks and $2N_2 = 379 \pm 31$ tracks, and from this we obtain (for the 14.8 and 17.6 MeV components together):

$$A = 0.14 \pm 0.09 \text{ (mean statistical error)}$$

Summing up the above results, and taking the mean value for A by the different methods, the differential cross-section of the

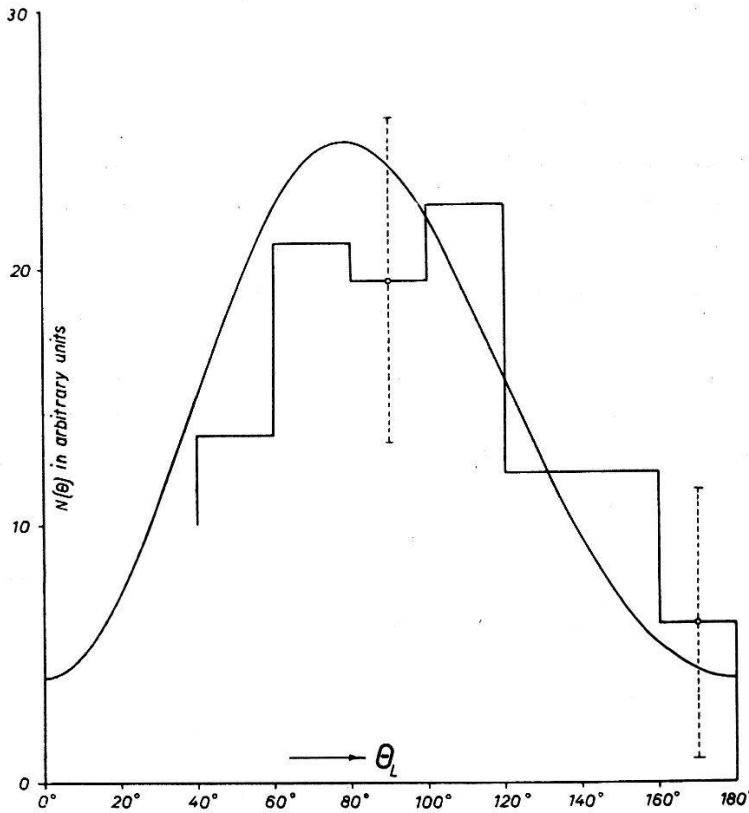


Fig. 15.

Angular distribution of the deuteron photo-disintegration for the 12,2 MeV gamma-rays (200 tracks in laboratory system).

deuteron photo-disintegration in the laboratory system is given by:

$$\sigma(\Theta) \sim (0.12 \pm 0.07) \cdot (1 + 0.14 \cos \Theta +) \sin^2 \Theta [1 + 0.54 \cos \Theta].$$

In addition, figure 15 gives the angular distribution in the laboratory system of photo-protons of the difference ($D_2O - H_2O$) grouped around 5.0 MeV which could be represented by:

$$\sigma(\Theta) \sim (0.2 \pm 0.2) + \sin^2 \Theta [1 + 0.45 \cos \Theta]$$

This qualitative result makes it also probable that the tracks of the difference ($D_2O - H_2O$) around 5 MeV arise from the deuteron photo-disintegration by a ≈ 12 MeV line.

(c) *Total cross-section.*

To calculate the cross-section of the $D(\gamma, n)p$ -reaction, let N_{eff} be the difference between the measured number of tracks in the D_2O and H_2O plates, respectively, corrected for the absorption of the gamma-rays. This number does not yet represent the total number of reactions occurring in the plate, due to the fact that some of the tracks will escape. Let ξ be the escape factor, to be multiplied by N_{eff} to get the true total number of reactions in the emulsion.

The total cross-section is then given very nearly by:

$$\sigma = \frac{4 \pi \cdot N_{\text{eff}} \cdot \xi \cdot d_1 \cdot d_2}{Z \cdot \delta \cdot n \cdot F}$$

where Z is the total number of gamma quanta emitted during the exposure, δ the thickness of the emulsion, n the number of the deuteron nuclei per cm^3 , F the scanned area of the plate and d_1 , d_2 are the distances between the source and the edges of the tested area opposing the source (see figure 2).

To compute ξ for an emulsion of thickness $2H$, one has to multiply the differential cross-section by the escape factor K and to integrate over the angle Θ . As the result of this integration, one gets

$$\xi = \frac{\frac{4}{3} + 2A}{\frac{H}{l} \left[1 + 2A + \frac{2}{3} \left(\frac{H}{l} \right)^2 \right]} \quad \text{for } l \geq 2H$$

and

$$\xi = \frac{\frac{2}{3} + A}{\frac{2}{3} + A - \frac{l}{H} \left(\frac{A}{4} + \frac{3}{16} \right)} \quad \text{for } l \leq 2H$$

where $A = 0.12$ is the isotropic constant in the differential cross-section. By multiplying each energy-interval by the appropriate factor ξ and summing up for all proton energies which belong to the two main lines (e. g. between 5.4 and 9.0 MeV), the product $N_{\text{eff}} \cdot \xi$ has been obtained. For each plate $\sigma_{\text{tot}} \{D(\gamma, n)p\}$ from the 14.8 and 17.6 MeV together was calculated separately and a weighed statistical mean has been considered:

$$\begin{aligned} \text{Mean } \sigma_{\text{tot}} (\text{from 14.8 and 17.6}) &= \frac{\sigma(14.8) I_1 + \sigma(17.6) I_2}{I_1 + I_2} \\ &= \underline{(8.34 \pm 1.0) \times 10^{-28} \text{ cm}^2} \end{aligned}$$

In this formulae, I_1 and I_2 are the relative numbers of quanta for the 14.8 and 17.6 MeV components respectively. The error mentioned includes statistical as well as systematical errors arising from the restricted number of tracks and the errors in plate scanning, as mentioned before. It does not yet include the uncertainty of the absolute intensity of the gamma-rays.

The ratio of the two components is assumed to be: $I_1/I_2 = 0.45$. Since all theories give at higher energies $\sigma(h\nu) \sim \frac{(h\nu - \varepsilon)^{3/2}}{(h\nu)}$ one can calculate σ_{tot} (14.8) and σ_{tot} (17.6) separately:

$$\begin{aligned}\sigma_{\text{tot}}(14.8) &= (8.7 \pm 2) \cdot 10^{-28} \text{ cm}^2 \\ \sigma_{\text{tot}}(17.6) &= (7.1 \pm 1.5) \cdot 10^{-28} \text{ cm}^2\end{aligned} \quad (\text{error limit})$$

The errors in σ_{tot} now contain also the uncertainty of the absolute intensity of the gamma-rays, which is estimated to be about 10%.

5. Discussion and comparison with the theory.

Although the statistics is by far improved yet the error is still not small enough to enable us to make an easy decision about the theory, which in turn, has not yet been quite settled. Nevertheless some conclusions about the $N-P$ interaction could be drawn from the present work. To sum up, table 1 gives the results of all published measurements together with the most important theoretical calculations for the isotropic constant A in the differential cross-section and of the total cross-section, at a gamma-ray energy of ~ 17.5 MeV.

Table 1.

Experiment			Theory		
Author	$\sigma \times 10^{28} \text{ cm}^2$	A	Author	$\sigma \times 10^{28} \text{ cm}^2$	A
Present work (2000 tracks)	7.1 ± 1.5	$0.12 \pm 0.07^*)$	BETHE ²³⁾ (central)	6.0	0.01
WILKINSON et al ⁹⁾	7.7 ± 0.9		HU & MASSEY ⁵⁾ (Charged)	7.4	0.07
FULLER ¹⁰⁾ (550 tracks)		$0.23^{**})$	(Neutral)	4.5	0.20
HOUGH ²⁴⁾ (260 tracks)	7.2 ± 1.5	$0.02^*) + 0.14$ $- 0.02$	MARSHALL & GUTH ³⁾ (central) $k = 0.5$	6.7	0.02

*) Values of A are taken for 14.8 and 17.6 MeV Li- γ rays combined.

**) Error in A is not given.

The value of our total cross section is very close to the results of the other authors mentioned in table 1. It is also in good agreement with the calculated electric dipole cross section, based on half ordinary and half exchange forces with an effective range $r_0 = 1.74 \times 10^{-13}$ cm⁶), and it rules out completely pure ordinary forces. It should furthermore be noted that the experimental cross sections indicated in table 1. contain also a contribution from non central forces, which makes the cross section for dipole transition still somewhat smaller.

Higher quantum energies would be needed to distinguish between the different possible shapes of the n-p potential.

As far as velocity independent forces are concerned, the most general potential of interaction between two nucleons at a distance r within the effective range r_0 currently has the form

$$V_{(12)} = -(1 - k + k P_x) \left\{ 1 + \frac{1}{2} g (\sigma_1 \cdot \sigma_2 - 1) + \gamma S_{12} \right\} V(r)$$

where $0 \leq k \leq 1$ is the mixing ratio, P_x is a space exchange operator, σ_1 and σ_2 are the PAULI spin operators of the two particles, S_{12} is the tensor force and $V(r)$ is the radial part of the nuclear potential. It is assumed that the three different potentials (the merely radial, the spin dependent and the tensor force) are of the same effective range r_0 but of depths proportional to $1 - \frac{1}{2} g$: $\frac{1}{2} g$: γ . The exchange operator P_x determines the value of V_{12} at higher l -states.

If one abandons the assumption of velocity independent forces, the introduction of a spin-orbit coupling, as it has been done by CASE and PAIS²⁵) would also give an isotropic constant in the angular distribution of the photo-protons.

The magnitude of the isotropic constant A in our angular distribution experiments indicates the presence of non central forces in the neutron-proton system. A force of this type would also give a good fit to the n-p scattering experiments at high energies²⁶).

Up to now, no extended calculations about the influence of different non-central interactions on the deuteron photo-disintegration have been published. (The calculation of its differential and total cross section by SCHIFF⁶) and by MARSHALL and GUTH³) are based on central mixed interaction ($\gamma = 0$ and $k = 0.5$) and consequently give no information about the magnitude of the isotropic constant A).

Since on the other hand different forms of the energy dependence of the isotropic constant A should be expected from different assumptions about non-central forces, further information — theoretical as well as experimental — concerning the angular distribu-

tion for different quantum energies would be very helpful in revealing the features of the n-p system.

We conclude from our results, combined with previous accurate ones from other authors, that the n-p interaction is of a mixed type ($\approx \frac{1}{2}$ ordinary and $\approx \frac{1}{2}$ exchange forces) with noncentral forces present. Moreover, the retardation effect postulated by MARSHALL and GUTH is confirmed.

To satisfy the situation about the parameters of the $N-P$ interaction, more experiments on the deuteron photo-disintegration with higher accuracy should be done. Further work on this subject with Lithium gamma-rays as well as Bremsstrahlung from a 32 MeV Betatron is in progress.

It is a pleasure for us to express our gratitude to Prof. Dr. P. SCHERRER, director of this institute, for his continuous interest in this work.

References.

- 1) J. CHADWICK and M. GOLDHABER: *Nature* **134**, 237 (1934); *Proc. Roy. Soc. A* **151**, 479 (1935).
- 2) A summary of results of previous published work has been given by C. H. COLLIE, H. HALBAN and R. WILSON, *Proc. Phys. Soc. A* **63**, 994 (1950).
- 3) J. F. MARSHALL and E. GUTH, *Phys. Rev.* **76**, 1879 (1949); *Phys. Rev.* **78**, 738 (1950).
- 4) W. RARITA and J. SCHWINGER, *Phys. Rev.* **59**, 556 (1941).
- 5) T.-M. HU and H. S. W. MASSEY, *Proc. Roy. Soc. A* **196**, 135 (1949).
- 6) L. I. SCHIFF, *Phys. Rev.* **78**, 733 (1950).
- 7) H. WÄFFLER and S. YOUNIS, *Helv. Phys. Acta* **22**, 414 (1949).
- 8) R. L. WALKER and B. D. MACDANIEL, *Phys. Rev.* **74**, 315 (1948).
- 9) J. H. CARVER and D. H. WILKINSON, *Nature* **167**, 154 (1951).
- 10) E. G. FULLER, *Phys. Rev.* **79**, 303 (1950); *Phys. Rev.* **76**, 576 (1949).
- 11) J. R. RICHARDSON and L. E. EMO, *Phys. Rev.* **53**, 234 (1938); R. W. BERRIMANN, *Nature* **162**, 992 (1948).
- 12) W. M. GIBSON, L. L. GREEN and D. L. LIVESSEY, *Nature* **160**, 534 (1947).
- 13) O. HIRZEL and H. WÄFFLER, *Helv. Phys. Acta* **20**, 373 (1947).
- 14) W. A. FOWLER, C. C. LAURITSEN and T. LAURITSEN, *Rev. mod. Physics* **20**, 236 (1948).
- 15) H. WÄFFLER and S. YOUNIS, *Helv. Phys. Acta* **22**, 614 (1949).
- 16) J. ROTBLAT and C. T. TAI, *Nature* **164**, 835 (1949).
- 17) W. M. GIBSON, *Proc. Phys. Soc. A* **62**, 586 (1949).
- 18) L. L. GREEN and W. M. GIBSON, *Proc. Phys. Soc. A* **62**, 407 (1949).
- 19) H. WÄFFLER, *Helv. Phys. Acta* **23**, 239 (1950).
- 20) C. M. G. LATTES, P. H. FOWLER and P. CÜER, *Proc. Phys. Soc. A* **59**, 883 (1947).
- 21) R. L. WALKER and B. D. MCDANIEL, *Phys. Rev.* **74**, 315 (1948).
- 22) H. A. BETHE, *Elementary Nuclear Theory* (John Wiley & Sons, N. Y. 1947).
- 23) P. V. C. HOUGH, *Phys. Rev.* **80**, 1069 (1950).
- 24) K. M. CASE and A. PAIS, *Phys. Rev.* **80**, 203 (1950).
- 25) B. S. CHRISTIAN and E. W. HART, *Phys. Rev.* **77**, 441 (1950).
- 26) H. NABHOLZ, P. STOLL and H. WÄFFLER, *Phys. Rev.* **82**, 963 (1951).